Biochimica et Biophysica Acta, 1056 (1991) 64–70
Elsevier

BBABIO 43310

Electrochromism of chlorophyll *a* monomer and special pair dimer

S. Krawczyk

Institute of Physics, M. Curie-Skłodowska University, Lublin (Poland)

(Received 7 May 1990)

Key words: Electrochromism: Chlorophyll *a* monomer; Special pair; Charge transfer; P700; Stark effect

The quadratic Stark effect was measured for chlorophyll monomer and dimer (Chl · ethanol)$_2$ in isotropic glassy solutions at low temperatures. The change in the permanent dipole moment, $\Delta\mu$, of chlorophyll monomer on excitation in the red absorption maximum was found to be (1.02 ± 0.09) D for both mono- and disolvate. It forms an angle $\delta = 20°$ with the electronic transition moment Q_y. The electronic excitation of the dimer within its main absorption band at 703 nm is accompanied by the change in dipole moment $\Delta\mu$ = (5.17 ± 0.2) D, for which $\delta = 23°$. A remarkable contribution from polarizability change, $\Delta\alpha$, to Stark spectra of both monomer and dimer was found within the Q_y band. In the monomer, $\Delta\alpha$ is several times higher in the region of vibrational side bands, where it is related to the second electronic transition (Q_x). The large increase in $\Delta\mu$ for the dimer as compared to the monomer is ascribed to charge-transfer contribution to the dimer excited state, due to significant overlap of electronic densities in the constituent monomers.

Introduction

Among the essential factors determining the primary charge separation in photosynthesis are the properties of electronic excited states of reaction center pigments The structures of bacterial reaction centers repeatedly confirm the dimeric nature of the primary electron donor which is composed of two BChl molecules with partly overlapping macrocyclic rings [1,2]. Theoretical studies on these structures [3,4] predicted a significant contribution from charge-transfer states to the lowest electronic transition in the excited state in these dimers and this was confirmed directly by measuring the Stark effect in bacterial reaction centers [5–8]. The asymmetric charge distribution between the primary donor constituents in its singlet excited state, at least partly determining the rate and directionality of the first electron transfer step, is retained also in its triplet state [9].

In relation to photosynthesis in higher plants and algae, a very similar 'special pair' (SP) dimer structure (Chl · L)$_2$ (where L is a bifunctional ligand such as water or alcohol) has been proposed for P700, the primary electron donor in PS I [10,11]. The basic spectral characteristics of this model SP dimer are analogous to those of P700 [12]. There is a large similarity between the deduced [11] and calculated [13] SP dimer structure and the primary electron donor in bacteria. In the light of accumulating evidence for dimeric structure of P700 [14], this makes the SP dimer a very plausible model for reference studies on the electronic properties that might be expected for P700.

This work deals with changes of permanent dipole moment and polarizability on electronic excitation in chlorophyll *a* monomers and in SP dimer, detected by investigating the Stark effect in the red region of the Chl absorption spectrum. The excitation of the dimer is accompanied by a large increase in the permanent dipole moment, which is an indicative of a considerable mixing of charge-transfer and exciton states. The comparison of electrochromic and absorption spectra has also proved to be helpful in establishing the position of the Q_x band in monomeric monosolvates of chlorophyll *a*.

Methods

The pigments were extracted and purified by high-performance liquid chromatography as previously described [15]. The solvents used, except for ethanol (99.8%) were distilled and dried over molecular sieves. Sample preparation included codistillation from dry carbon tetrachloride [16] and dissolving Chl in dry solvent.

Correspondence: S. Krawczyk, Institute of Physics, M. Curie-Skłodowska University, 20-031 Lublin, Poland.

0005-2736/91/$03.50 © 1991 Elsevier Science Publishers B.V. (Biomedical Division)

The monochromatic light source consisted of a 0.4 m monochromator driven by a stepping motor and equipped with a 150 W halogen lamp. The light transmitted by the sample was detected by a silicon photodiode and its AC component was amplified and phase detected at the second harmonic frequency of the cuvette voltage (960/1920 Hz). Both AC and DC components were digitized and recorded simultaneously at 10 or 20 cm^{-1} intervals and numerically converted to ΔA and to the absorbance A (reference records with solvent-filled cuvette were used in the latter case). Since the reflectance of the cuvette walls did not exceed 10%, no corrections were introduced to account for multiple reflections.

The cuvette was placed in a transparent Dewar flask attached to a cryostat which provided nitrogen vapor of variable temperature. The sample temperature was controlled seperately. A polarizing foil was glued flat to the internal wall of the Dewar flask; it might be placed in or removed from the light beam by rotating the flask. The angle of incidence (and thus the angle χ, cf. Eqn. 1) was varied by rotating the sample around the vertical axis by up to 55° in horizontally polarized light.

The cuvettes were prepared from glass plates coated with conducting SnO_2 layers. The spacing of the plates, typically 0.05–0.06 mm, was provided by Teflon foil with a window (10 × 25 mm) pressed between them. Sample solutions were applied to the cuvette through small holes drilled in one of the glass walls and in the stainless steel cover equipped with Teflon screw stoppers. The thickness of the cuvette was determined by placing an empty cuvette in the apparatus perpendicularly to the monochromatic light beam (1 × 6 mm cross-section) and by applying 500 V AC voltage. A weak modulated signal in the transmitted light, presumably due to electrostatic attraction of the cuvette walls, was detected at the second harmonic frequency of the applied voltage. Sweeping the wavelength revealed the appearance of interference fringes whose spacing, about 5 nm, was used to calculate the cuvette thickness.

Thin-layer chromatography and control recordings of the visible absorption spectrum of samples diluted with diethyl ether revealed no changes during the experiments.

All Stark spectra reported here were analysed by fitting them with the linear combination of the first and second derivatives of the absorption spectra, in accordance with the general formula for the quadratic Stark effect [17]:

$$\Delta A = \frac{1}{\sqrt{2}}\left\{\frac{\Delta\alpha}{2hc}\nu\frac{d(A/\nu)}{d\nu} + \frac{(\Delta\mu)^2}{10h^2c^2}\nu\frac{d^2(A/\nu)}{d\nu^2}\right.$$

$$\left.\times((3\cos^2\delta - 1)\cos^2\chi + 2 - \cos^2\delta)\right\}\cdot F^2 \qquad (1)$$

where $\Delta\mu$ and $\Delta\alpha$ denote, respectively, the differences of the permanent dipole moment and polarizability in the ground and excited state: $\Delta\bar{\mu} = \bar{\mu}_e - \bar{\mu}_g$, $\Delta\alpha = \alpha_e - \alpha_g$; A is the absorbance, ν the wavenumber, δ the angle between the transition dipole moment and $\Delta\bar{\mu}$, χ the angle between the effective electric field, F, and the electric vector of the light. The factor $1/\sqrt{2}$ accounts for detection of the second harmonic in the modulated light intensity. The value of δ was calculated from the slope of the plots of $\Delta A(\chi)/\Delta A(90°)$ vs. $\cos^2\chi$ [5] (the values of ΔA in the minimum corresponding to the main absorption band were used). The angle χ was calculated using the refractive index of the sample equal to 1.5. Then, $\Delta\bar{\mu}$ was calculated from the minimum of ΔA where the contribution from polarizability term (cf. Eqn. 1 and Figs. 1C, 2C) is zero.

The values of $\Delta\alpha$ were estimated from the coefficient at $\nu \cdot d(A/\nu)/d\nu$ in the linear least squares fit of Eqn. 1 to the Stark spectrum. Although the molecular polarizability is generally a tensor, it was assumed in this work to be a scalar. Thus, the values of $\Delta\alpha$ reported here are only rough estimates of a 'mean' polarizability change on electronic excitation.

In all experiments, a close proportionality of the Stark spectra to the square of the electric field strength up to $6.6 \cdot 10^4$ V/cm was confirmed.

Results

Chlorophyll monomers

The absorption and Stark spectra of monosolvate Chl with the Mg atom externally coordinated by triethylamine are shown in Fig. 1. Although the minimum in the Stark spectrum (Fig. 1B) coincides with the peak of the main absorption band $Q_y(0–0)$, fitting the spectrum with Eqn. 1 reveals a significant contribution from the change in molecular polarizability, $\Delta\alpha$, in addition to the $\Delta\mu$ term. Also, the entire Stark spectrum can not be fitted with Eqn. 1 using single values for $\Delta\mu$ and $\Delta\alpha$. Adjusting the coefficients at the first and second derivatives (cf. Eqn. 1) in different parts of the spectrum shows that there are two regions where satisfactory fits can be obtained: one of them is the region of the main $Q_y(0–0)$ absorption band and the other covers the first vibrational side band $Q_y(0–1)$ between 15 500 and 16 500 cm^{-1}. They differ mainly in the polarizability contribution : in the region of $Q_y(0–1)$, $\Delta\mu$ is typically larger by a factor of 1–1.2, while $\Delta\alpha$ increases 3–7-times relative to its value in the $Q_y(0–0)$ band. The values of molecular parameters estimated are listed in Table I.

The variability of $\Delta\alpha$ along the spectrum is more evident in the Stark spectra of Chl disolvate. Fig. 2A shows the absorption spectrum of Chl with the magnesium atom coordinated on both sides of the porphyrin ring by tetrahydrofuran molecules. The splitting of bands above 15 500 cm^{-1} into four instead of normally

observed two bands is related to the Q_x band shift on six-coordination of the magnesium atom in chlorophyll *a* [18–20]. The coincidence of $Q_x(0–0)$ maximum with the inflexion point in the Stark spectrum, indicated by vertical line in Fig. 2, suggests that the main contribution to electrochromism comes from the term in Eqn. 1 related to polarizability, as the Stark spectrum in this region contains a prevailing contribution from the first derivative of the absorption spectrum (cf. Table I). In the $Q_y(0–0)$ band, however, the minimum in the Stark spectrum nearly coincides with the position of the absorption peak and only the asymmetry indicates contribution from $\Delta\alpha$ in addition to the dominating $\Delta\mu$ term. Although the appearance of overlapping Q_x and Q_y

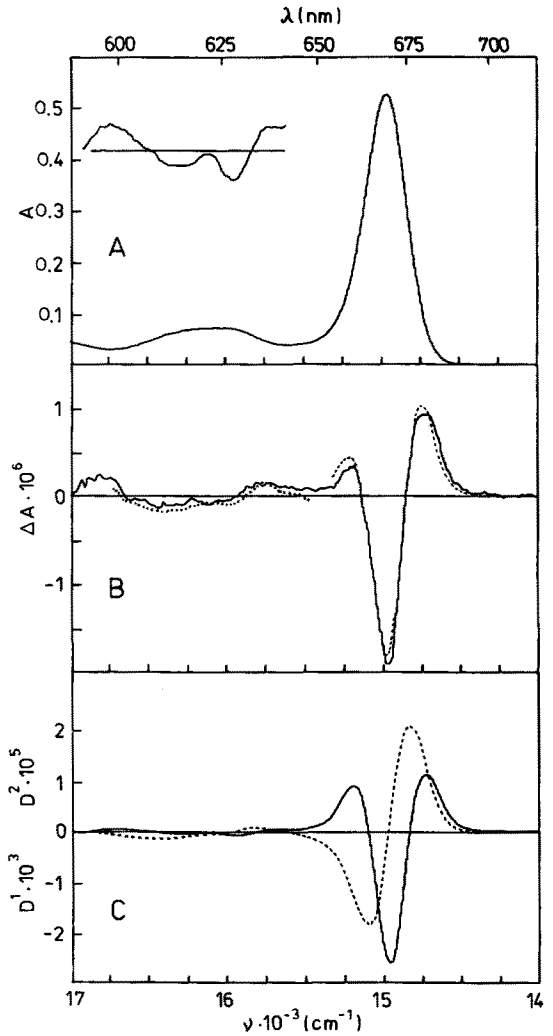

Fig. 1. Spectra of Chl *a* in 1:1 (v/v) mixture of ethylbenzene and butylbenzene containing 0.25 M triethylamine. (A) Absorption spectrum. Inset: the second derivative in the region of $Q_y(0–1)$ band (enlarged). (B) Stark spectrum (continuous line) and the fits of Eqn. 1 (dotted line). Fit parameters: $\Delta\mu = 0.97$ D, $\Delta\alpha = 2$ Å^3 from 14500 to 15300 cm^{-1}, and $\Delta\mu = 1.08$ D, $\Delta\alpha = 10$ Å^3 from 15500 to 16750 cm^{-1}. (C) The first (dotted line) and the second (continuous line) derivatives of the absorption spectrum. Temperature: 118 K, field strength (rms): $5.97 \cdot 10^4$ V/cm.

TABLE I

The wavelengths of the main bands in absorption and Stark spectra of Chl species studied, the change in permanent dipole moment $\Delta\mu$, and estimated polarizability changes $\Delta\alpha$

All samples except for Chl, in isopropanol, are in ethylbenzene/butylbenzene (1:1, v/v) plus ligand at concentration indicated. For explanation of $\Delta\alpha$ for the dimer see text. ta, triethylamine; tf, tetrahydrofuran; et, ethanol.

Chl species, solvent, temperature	Absorption maximum (nm)	Stark minimum (nm)	$\Delta\mu$ (Q_y) (D)	$\Delta\alpha$ (Å^3)
Monosolvate, ta 0.25 M 118 K	668.5	668	0.95	Q_y 2.2 $Q_x \cong 13$
Monosolvate, isopropanol, 155 K	666	665.5	1.09	Q_y 1.5 $Q_x \cong 5$
Disolvate, tf 0.4 M 118 K	669	668	0.92	Q_y 4 $Q_x \cong 30$
Dimer $(Chl \cdot et)_2$ 108–155 K	703	699.5	5.17	mean 93

bands above 15500 cm^{-1} makes a more detailed analysis difficult, it is clear from the above comparison that the apparent difference in electrochromism of $Q_y(0–0)$ and vibrational side-bands is due to the presence of Q_x bands overlapping with the latter. Similar effects related to Q_x bands were reported also for bacteriochlorophyll *a* and bacteriopheophytin *a* [6].

Special pair dimer

The absorption spectrum of a solution of chlorophyll *a* in nonpolar solvent in the presence of ethanol is shown in Fig. 3A (curve 1). The red-shifted absorption band at 703 nm appears on cooling and is due to the dimer $(Chl \cdot ethanol)_2$ [11,16]. In this dimer, each ethanol molecule binds simultaneously the Mg atom of one chlorophyll molecule and the keto C = O group of the other: (1, 2)Mg...O-H...O = C(2, 1). When the concentration of ethanol is much higher, chlorophyll is almost completely converted into monomeric form due to competitive hydrogen bonding of five-coordinated ethanol and of the keto groups of Chl by other ethanol molecules. The absorption spectrum of monomeric monosolvate (Chl · ethanol) is also shown in Fig. 3A (top spectrum, curve 2).

The dotted line in Fig. 3B is the Stark spectrum of the sample represented by curve 1 in Fig. 3A. The pure Stark spectrum of the dimer can be obtained in two ways. The first is based on calculating the second derivative of the absorption spectrum within the monomer band at 14900 cm^{-1} scaling it with the $\Delta\mu$ for monomer and subtracting it from the crude Stark spectrum. The second way is to assume an approximate value for monomer absorption and to use it for scaling a Stark

spectrum of the monomer to be subtracted. Both procedures resulted in similar small corrections in the range 14700–15200 cm^{-1}. The true electrochromism of the dimer is represented by continuous line in Fig. 3B.

The Stark spectrum of the dimer exhibits a very strong negative band whose shape resembles the second derivative of dimer's absorption band. It can be inferred from Fig. 3A that the absorption of monomeric chlorophyll does not appreciably interfere with the dimer band below 14500 cm^{-1} (690 nm). The values of $\Delta\mu$ for the dimer band at 703 nm (14230 cm) are 5-times larger than for monomeric chlorophyll and equal to (5.17 ± 0.2) D. This value is well reproducible; it was found the same with samples containing diverse proportions of dimers and monomers. Following theoretical predictions [21], this large increase in the permanent dipole moment is postulated to reflect the charge-transfer character of the excited (Franck-Condon) state of the dimer, in analogy with the dimeric bacterial primary donors P870 and P960 [5–8].

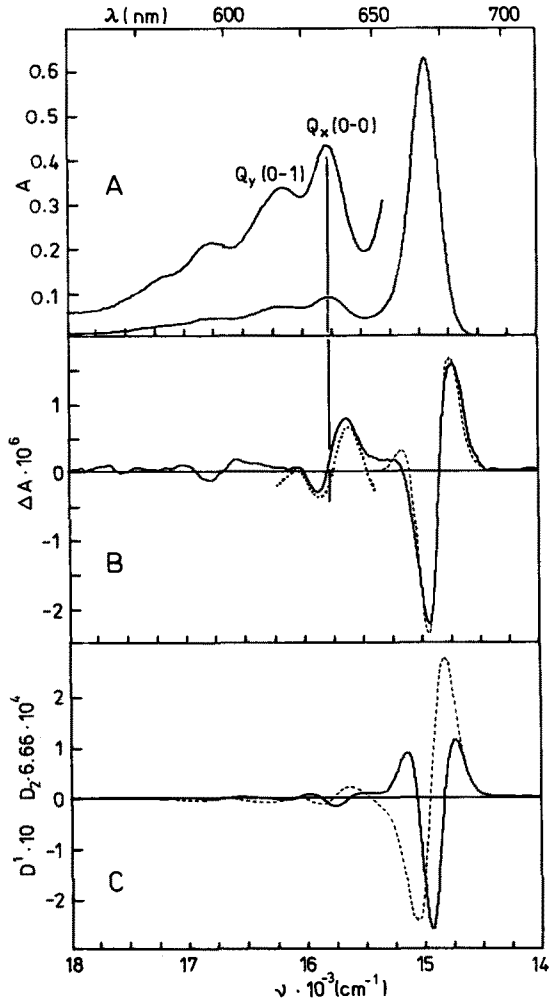

Fig. 2. Spectra of Chl *a* in 1:1 (v/v) ethylbenzene/butylbenzene in the presence of 0.4 M tetrahydrofuran. (A) Absorption; (B) Stark spectrum (continuous line) and the fit of Eqn. 1 (dotted line). Fit parameters: $\Delta\mu = 0.95$ D, $\Delta\alpha = 3.3$ Å^3 from 14500 to 15300 cm^{-1}, and $\Delta\mu = 0.82$ D, $\Delta\alpha = 36$ Å^3 from 15400 to 16250 cm^{-1}. (C) The first (dotted line) and the second (continuous line) derivatives of absorption. Temperature: 118 K, field strength (rms): $6.27 \cdot 10^4$ V/cm.

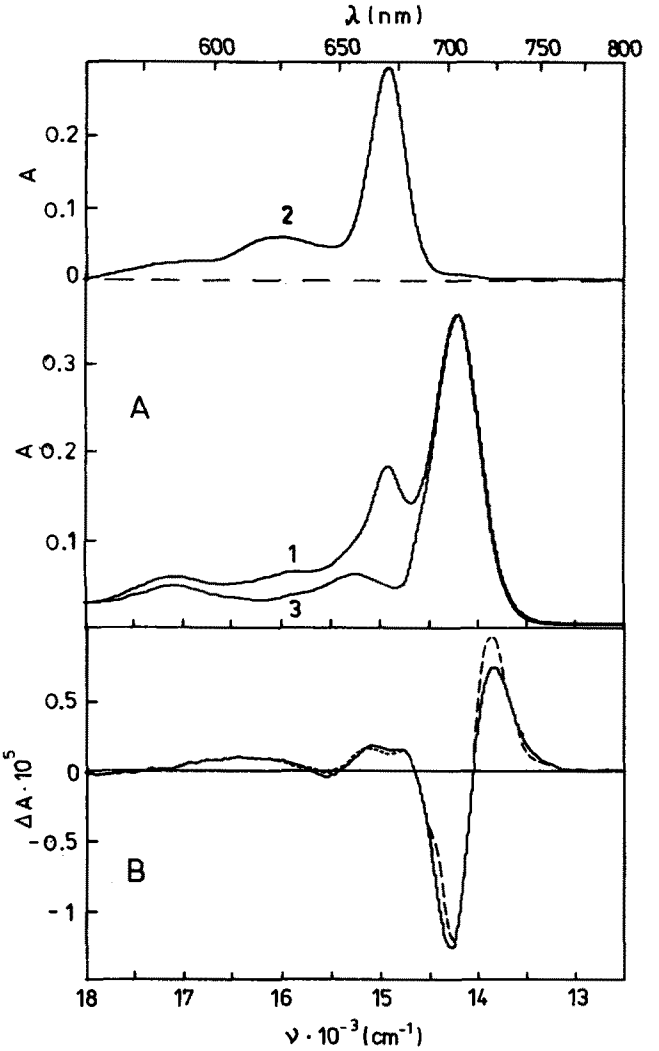

Fig. 3. (A) Absorption spectra of Chl *a* in ethylbenzene/butylbenzene (1:1, v/v) with ethanol. (1) Absorption spectrum of a sample with nominal Chl concentration $1.1 \cdot 10^{-3}$ M in the presence of $5 \cdot 10^{-3}$ M ethanol; (2) absorption spectrum of monomer obtained at $5 \cdot 10^{-2}$ M ethanol concentration in a separate experiment; (3) approximate absorption spectrum of the dimer resulting from subtraction of scaled curve 2 from 1. (B) Dotted line – the Stark spectrum of the sample represented by curve 1A (it overlaps with the continuous line in the remaining part of spectra); continuous line – corrected dimer spectrum; interrupted line – fit of Eqn. 1 (see text for details). Temperature 118 K, field strength, $6.27 \cdot 10^4$ V/cm.

Despite the presence of a small amount of monomeric chlorophyll, both the absorption and Stark spectra in the wavenumber range from 13000 to 14500 cm^{-1} are dominated by the dimer and seem to be quite adequate to make use of Eqn. 1. However, shifting the region of the spectrum to be fitted from 13000 cm^{-1} toward higher wavenumbers results in continuously increasing values of $\Delta\alpha$ from 65 Å^3 on the long-wavelength slope of the dimer absorption band to 125 Å^3 on

the short-wavelength side. At the same time, the fit quality becomes poorer, but the value of $\Delta\mu$ related to the second term in Eqn. 1 remains constant within 5%. The fitting curve for the whole region 13000–14500 cm^{-1} is represented by interrupted line in Fig. 3B. Being based on the 'mean' value of $\Delta\alpha$, it exhibits deviations of opposite sign on both slopes of the absorption band.

The origin of the Stark spectrum in the range 14500–18000 cm^{-1} becomes clear if appropriately scaled absorption spectrum of the monomer (Fig. 3A, top) is subtracted from the spectrum of the sample (curve 1 in Fig. 3A), until the sharp monomer band disappears. This procedure reveals a second band at about 15250 cm^{-1} (656 nm) attributable to the dimer absorption, which presence can be inferred directly from curve 1 in Fig. 3 where this band appears as a weak shoulder on the higher-frequency side of the monomer band. Although the shape and intensity of this band, obtained by somewhat arbitrary procedure, may be uncertain, its position remains essentially the same, independent of whether the scaling factor for the subtracted monomer band is increased or decreased by 20%. The coincidence of this band with the inflexion point in the Stark spectrum indicates a dominating effect of the polarizability change, $\Delta\alpha$, on the electrochromism in this range, as is also the case for the third band at 17100 cm^{-1} (585 nm).

Discussion

The values of both $\Delta\mu$ and $\Delta\alpha$ obtained here were calculated under assumption that the effective electric field, F, in Eqn. 1 is equal to the macroscopic field, F_m. As mainly nonpolar solvents were used at low temperatures, their dielectric constants may be assumed approximately equal to those at normal temperature. The observed consistence of $\Delta\mu$ for chlorophyll in frozen isopropanol solution with that in alkylbenzenes (see Table I) indicates that the correction for the local field is quite similar in both cases and is determined by electronic-vibrational polarizability of the solvent which can be approximated by the square of the refractive index. Thus, for isotropic solution, the Lorentz formula: $F = (\epsilon + 2)F_m/3$ gives the correction factor 0.715 which should be multiplied by $\Delta\mu$ and $\Delta\alpha$ values reported in Table I to obtain their values in vacuo. The value of $\Delta\mu \equiv 1$ D for monomeric Chl a, which is significantly smaller than the approx. 2.5 D reported for bacteriochlorophyll a [7], is in reasonable agreement with 0.46 D which may be deduced from theoretical ab initio calculations [22].

The Q_y and Q_x bands were found to contribute to the Stark spectrum through, respectively, $\Delta\mu$- and $\Delta\alpha$-based mechanisms. This observation provides an argument helpful in resolving the long-standing question concerning the position of $Q_x(0–0)$ band in absorption spectra of monosolvate chlorophyll a. This band was postulated either to lie at approx. 585 nm and overlap with the $Q_y(0–2)$ [18,23,24], or to lie at 620–625 nm and overlap with $Q_y(0–1)$ [20,25]. In disolvates, $Q_x(0–0)$ is always observed as a distinct peak at 620–625 nm in dioxane, tetrahydrofuran [18] and ethylene oxide [15] or at 639 nm in pyridine [18,19]. The strong contribution from $\Delta\alpha$ to the Stark spectra of chlorophyll monosolvate within $Q_y(0–1)$, like that in disolvate spectrum where $Q_x(0–0)$ appears as a distinct band, strongly suggests the overlap of $Q_x(0–0)$ with $Q_y(0–1)$. Also, the clear splitting in the second derivative shown in Fig. 1A indicates the composite nature of absorption spectrum in the region of $Q_y(0–1)$ band. It should be mentioned at this point that, although disolvation of chlorophyll is strongly enhanced in some solvents at low temperature, our previous resonance Raman data [15] have shown that chlorophyll retains the five-coordinated state in neat triethylamine at 77 K. This definitely rules out the possibility of disolvation in 0.25 M triethylamine used here.

Within the framework of exciton theory, the main dimer band at 703 nm is related to a single electronic transition to the P_- exciton state of the two antiparallel Q_y transition moments of the monomers [11]. Early calculations on chlorophyll a [21] and bacteriochlorophyll a [26] dimers of similar structure but with translational symmetry predicted significant bathochromic shift of the dimer absorption band in the red, resulting from the overlap of electron densities in the monomers which gives rise to charge-transfer states that mix with the exciton states. This was later investigated theoretically mainly in relation to the primary donor in bacterial photosynthesis, consisting of bacteriochlorophyll molecules [3,4]. Our results for model SP dimer of chlorophyll a agree with these predictions, in analogy with partial charge-transfer character of the lowest electronic transition in bacterial primary donor dimers [5–8]. Also, the value of angle $\delta = 23°$ is very close to the angle between the transition moment and the line connecting the centers of both molecules, estimated to be about 24° [11].

There is, however, one remarkable difference. For the Chl a dimer studied here, the Stark spectrum evidently does not follow Eqn. 1 exactly and a variable contribution from either $\Delta\alpha$ or $\Delta\mu$ must be introduced to fit the experimental data. This discrepancy was invariably observed over the whole temperature range, 108–155 K; thus, the possibility of some contribution from orientational effects in the electric field should be excluded, as the viscosity of the glassy solvent depends on the temperature. Moreover, the trials to fit the Stark spectrum with a linear combination of the absorption spectrum and its first and second derivatives resulted in good fits in which the contribution from the absorption spectrum was negative, i.e., opposite to what can be expected

from orientational effect when the transition moment is nearly perpendicular to $\bar{\mu}_g$ [22].

The remarkable contribution from the change in polarizability to Stark spectra of both monomer and dimer of chlorophyll *a* can be explained by field-induced mixing of excited states [28]. For a molecule having two closely lying excited states 1 (the lowest) and 2 (higher in energy) but well separated from the other states on the energy scale, the shift in energy of the lower state in the electric field F is always negative and it can be shown to be given by:

$$\Delta E_1 = -\frac{|\langle 1|W|2\rangle|^2}{E_2 - E_1} \tag{2}$$

where $W = -\bar{p}\cdot\bar{F}$ and $\bar{p}$ is the dipole moment operator. The proportionality of ΔE_1 to F^2 is equivalent to a polarizability term and thus we have:

$$\Delta\alpha = \frac{2|\langle 1|\bar{p}|2\rangle|^2}{3(E_2 - E_1)} \tag{3}$$

(the number 3 in the denominator accounts for isotropic orientation of molecules). Estimation of $\Delta\alpha$ for $Q_y(0\text{–}0)$ as the state 1 and $Q_x(0\text{–}0)$ (state 2) with $E_2 - E_1 \cong 1000$ cm^{-1} and $\langle 1|p|2\rangle \cong 1$ D * gives $\Delta\alpha \cong 3$ Å. This result suggests that, in the case of chlorophyll *a* monomers, the experimentally estimated values of $\Delta\alpha$ for the $Q_y(0\text{–}0)$ band (cf. Table I) can be fully accounted for by the presence of the $Q_x(0\text{–}0)$ band. In the case of the $Q_x(0\text{–}0)$ band, the calculation should include also its overlap with $Q_y(0\text{–}1)$ which is now higher in energy than Q_x and much closer to it; this circumstance points to a higher polarizability of the $Q_x(0\text{–}0)$ band than that estimated for $Q_y(0\text{–}0)$, in agreement with my experimental data.

In the dimer, the charge transfer state combines with both 'plus' and 'minus' states (although differently [4]), adding to $\bar{p}$ a component that increases the matrix element in Eqn. 3 for the lowest P_- state, in addition to the effect of higher-lying P_+ state and those originating from Q_x transitions. This can qualitatively explain the large value of $\Delta\alpha$ for the lowest electronic transition in chlorophyll dimer.

The electrochromism on the short-wavelength slope of the dimer band is too strong to be accounted for by the first-derivative term in Eqn. 1. This deviation, as well as the large value of $\Delta\alpha$ itself, can in principle result from possible inhomogeneity in stable dimer structures (i.e., different interplanar distances and angles), each with different charge transfer contribution. However, it must be taken into account that the degree of mixing is the main factor determining the band shift to the red [21]; thus, the possible higher-energy band(s) should be related with rather weaker electrochromism, contrary to what is observed. Another possibility is the participation of highly excited low-frequency phonon modes (including intermolecular coordinates) in the excited Franck-Condon P_- state. The involvement of electron-phonon coupling into P_- transitions of reaction center dimers (both bacterial and P700) has been postulated on the basis of large values of the Huang-Rhys factor $S \cong 7$ in the hole-burning spectra [27]. Although more evidence points to this explanation, more must be known about the band structure of the dimer spectrum and the band-shifting effect of the electric field before a definitive conclusion is reached.

The origin of the second dimer band, at 15 250 cm^{-1}, is not obvious. It can be (i) the exciton P_+ band related to Q_y transitions in monomers, (ii) an exciton band originating from Q_x transitions in monomers, or (iii) the vibrational band of the dimer. Its weak electrochromism, determined mainly by the change in polarizability, does not exclude the first possibility. A very weak absorption intensity (1:20) was predicted theoretically for the higher-energy exciton transition mixed with charge-transfer state in dimers of translational symmetry with parallel Q_y transition moments [21], in accordance with expectations based on pure exciton theory. If the Q_y transitions would be not perfectly antiparallel in the dimer considered here and the P_+ transition had a noticeable intensity at 15 250 cm^{-1}, its much weaker electrochromism could be consistent with its weaker mixing with the charge transfer state [4]. The second possibility will be ruled out because of generally low intensity of the Q_x band in five-coordinated monomers. Additionally, the exciton splitting of Q_x transitions is expected to produce rather a higher-energy band as their transition dipole moments are perpendicular to the vector connecting the centers of both monomers. Although intensity gain arising from the coupling of Q_x transitions to other electronic states can not be excluded, we suggest the assignment of the dimer band at $\cong$ 15 250 cm^{-1} to the P_+ state or to a vibrational satellite of P_-. The latter assignment is in an approximate agreement with the typical $\cong$ 1000 cm^{-1} spacing of this band from P_-, like in chlorophyll monomers, while the former would be plausible for explaining the large polarizability contribution to the Stark effect in P_- according to the mechanism discussed above.

There are several types of chlorophyll aggregation state that give rise to the appearance of long-wavelength bands. They are the chlorophyll-water adducts of different size, absorbing at $\cong$ 730 nm [29], and Langmuir-Blodgett multilayer films which absorption spectra in the red exhibit a shoulder extending to 720 nm [30–32]. In one case [30], an enhanced electrochromism of Chl *a* in multilayers was observed at 700 nm, which

* For comparison, the dipole strengths for Q_y and Q_x transitions are, respectively, 22.4 D^2 and 3.5 D^2 [24].

was ascribed to some specific orientation of transition moments in Chl aggregate.

The presence of the long-wavelength-absorbing species depends critically on the water content in the multilayer [32]. This observation, together with the results of the present work and in conjunction with Stark effect spectroscopy of chlorophyll in Langmuir-Blodgett films [30], reveals a widespread occurrence of charge-transfer transitions in aggregates of stacked chlorophyll molecules linked by bifunctional ligands.

Acknowledgement

This work was performed under contract R.P.II.11. 1.5.

References

1 Deisenhofer, J., Epp, O., Miki, K., Huber, R., and Michel, H. (1985), Nature 318, 618–624.
2 Yeates, T.O., Komiya, H., Chirino, A., Rees, D.C., Allen, J.P. and Feher, G. (1989) Nature 339 111–116.
3 Warshel, A. .and Parson, W.W. (1987) J. Am. Chem. Soc. 109, 6143–6152.
4 Parson, W.W. and Warshel, A. (1987) J. Am. Chem. Soc. 109, 6152–6163.
5 Lösche, M., Feher, G. and Okamura, M.Y. (1987) Proc. Natl. Acad. Sci. USA 84, 7537–7541.
6 Lockhart, D.J. and Boxer, S.G. (1987) Biochemistry 26, 664–668.
7 Lockhart, D.J. and Boxer, S.G. (1988) Proc. Natl. Acad. Sci. USA 85, 107–111.
8 Boxer, S.G., Goldstein, R.A., Lockhart, D.J., Middendorf, T.R. and Takiff, L. (1989) J. Phys. Chem. 93, 8280–8294.
9 Norris, J.R., Budil, D.E., Cast, P., Chang, C.-H., El-Kabbani, O. and Schiffer, M. (1989) Proc. Natl. Acad. Sci. USA 86, 4335–4339.
10 Boxer, S.G. and Closs, G.L. (1976) J. Am. Chem. Soc. 98, 5406–5408.
11 Shipman, L.L., Cotton, T.M., Norris, J.R. and Katz, J.J. (1976) Proc. Natl. Acad. Sci. USA 73, 1791–1794.
12 Katz, J.J., Shipman, L.L. and Norris, J.R. (1979) Ciba Found. Symp. 61, 1–40.
13 Kashiwagi, H., Hirota, F., Nagashima, U. and Takada, T. (1986) Int. J. Quant. Chem. 30, 311–326.
14 Lagoutte, B. and Mathis, P. (1989) Photochem. Photobiol. 49, 833–844.
15 Krawczyk, S. (1989) Biochim. Biophys. Acta 976, 140–149.
16 Cotton, T.M., Loach, P.A., Katz, J.J. and Ballschmiter, K. (1978) Photochem. Photobiol. 27, 735–749.
17 Reich, R. and Schmidt, S. (1972) Ber. Bunsenges. physik. Chem. 76, 589–598.
18 Seely, G.R. and Jensen, R.G. (1965) Spectrochim. Acta 21, 1835–1845.
19 Evans, T.A. and Katz, J.J. (1975) Biochim. Biophys. Acta 396, 414–426.
20 Renge, I. and Avarmaa, V. (1975) Photochem. Photobiol. 42, 253–260.
21 Warshel, A. (1979) J. Am. Chem. Soc. 101, 744–746.
22 Petke, J.D., Maggiora, G.M., Shipman, L. and Christoffersen, R.E. (1979) Photochem. Photobiol. 30, 203–223.
23 Houssier, C. and Sauer, K. (1970) J. Am. Chem. Soc. 92, 779–791.
24 Shipman, L.L., Cotton, T.M., Norris, J.R. and Katz, J.J. (1976) J. Am. Chem. Soc. 98, 8222–8230.
25 Belkov, M.V. and Losev, A.P. (1978) Spectr. Lett. 11, 653–659.
26 Warshel, A. (1980) Proc. Natl. Acad. Sci. USA 77, 3105–3109.
27 Gillie, J.K. Fearey, B.L., Hayes, J.M. and Small, G.J. (1987) Chem. Phys. Lett. 134, 316–322.
28 Scherer, P.O.J. and Fischer, S.F. (1986) Chem. Phys. Lett. 131, 153–159.
29 Ballschmiter, K. and Katz, J.J. (1969) J. Am. Chem. Soc. 91, 2661–2677.
30 Kleuser, D. and Bücher, H. (1969) Z. Naturforsch. 24b, 1371–1374.
31 Désormeaux, A. and Leblanc, R.M. (1985) Thin Solid Films 132, 91–99.
32 Krawczyk, S., Leblanc, R.M. and Marcotte, L. (1989) J. Chim. Phys. 85, 1073–1078.